**SUPPLEMENTARY INFORMATION**

# Structure-function evolution of transition metal molybdate catalysts driven by hydrodeoxygenation environment

Gabriel B. Báfero[1a], Guilherme B. Strapasson[1,2], Leonardo S. Sousa[1b], James S. Hayward[3], Pedro B. M. Nunes[1], Davi S. Leite[1], David J. Morgan[3,4], Jonathan K. Bartley[3]*, Daniela Zanchet[1]*

[1] *Institute of Chemistry, University of Campinas (UNICAMP), Campinas, 13083-970, BR.*

[2] *Brazilian Synchrotron Light Laboratory (LNLS), Brazilian Center for Research in Energy and Materials (CNPEM), Campinas, 13083-100, BR.*

[3] *Cardiff Catalysis Institute (CCI), School of Chemistry, Cardiff University, Cardiff, CF10 3AT, UK.*

[4] *HarwellXPS, Research Complex at Harwell (RCaH), Didcot, OX11 OFA, UK.*

* corresponding authors: bartleyjk@cardiff.ac.uk, zanchet@unicamp.br

Present addresses:

[a] *Brazilian Synchrotron Light Laboratory (LNLS), Brazilian Center for Research in Energy and Materials (CNPEM), Campinas, 13083-100, BR.*

[b] *Research Complex at Harwell (RCaH), Rutherford Appleton Laboratory, Harwell Science and Innovation Campus, Didcot, OX11 0FA, UK.*

## Characterization Methods

**X-ray Diffraction.** X-ray diffraction (XRD) measurements were obtained using a Panalytical X'pert Pro diffractometer using Cu Kα X-ray source operating with an accelerator voltage 40 kV and 40 mA current. XRD powder patterns were recorded over a 2θ range of 20-60°. The obtained diffractograms were compared to reference patterns from the Inorganic Crystal Structure Database (ICSD).[1] The crystallite sizes of the CuMo catalyst and the subsequent phases formed after the acetone HDO reaction were estimated using the Scherrer equation. For the $Cu_3Mo_2O_9$ phase, the XRD peaks corresponding to the (200) and (131) reflections were used; for the MoC phase, the (111) and (200) reflections; and for metallic $Cu^0$, the (111) and (200) reflections.

**X-ray Fluorescence.** Elemental composition of fresh and post-reaction MMo catalysts was semi-quantitatively analyzed using a Shimadzu energy dispersive micro X-ray fluorescence spectrometer, μEDX-1300 (S/N Q20644200016, Kyoto, Japan). For each sample, five different points were analyzed, with an irradiation area of 50 μm in diameter per point. Spectral interpretation and elemental quantification (for detectable and measurable elements with atomic number $Z \geq 12$) were carried out based on the fundamental parameters method.

**X-ray Photoelectron Spectroscopy.** Quantitative elemental composition and oxidation state analysis of fresh and post-reaction MMo catalysts were performed using a Kratos Axis Ultra DLD system was used to collect XPS spectra using monochromatic Al Kα X-ray source operating at 120 W (10 mA × 12 kV). Data was collected with pass energies of 160 eV for survey spectra, and 40 eV for the high-resolution scans with step sizes of 1 eV and 0.1 eV respectively. The system was operated in the hybrid mode, using a combination of magnetic immersion and electrostatic lenses, and acquired over an area approximately 300 × 700 $\mu m^2$. A magnetically confined charge compensation system using low energy electrons was used to minimize charging of the sample surface, and all spectra were taken with a 90° take of angle. A pressure of ca. $5\times10^{-9}$ Torr was maintained during collection of the spectra. Before insertion into the system, samples were pressed on to silicone-free double-sided adhesive tape attached to a cut glass slide into flatted using a second, isopropyl alcohol cleaned glass microscope slide. All data was analysed using CasaXPS (v2.3.26) after subtraction of a Shirley background and

using modified Wagner sensitivity factors as supplied by the instrument manufacture.[2] Where required, fitting was performed using Voigt-like functions using the LA function in CasaXPS.

It is important to highlight that the interpretation of Mo 3d XPS spectra in transition MMo requires careful consideration of chemical environment effects. This region is notoriously complex due to atypical line shapes and binding-energy (BE) shifts arising from crystalline vs. amorphous oxides and final-state screening.[3] To track treatment-induced changes, we analysed a set of *ex situ* spectra using a linear-algebra approach.[3,4] All spectra were calibrated to the lattice Mo-O O 1s at 530.5 eV (average across Mo oxides; NIST SRD-20), which placed $Mo^{6+}$ ($3d_{5/2}$) at 232.4 ± 0.2 eV, consistent with $MoO_3$.[5]

Pure $MoO_2$ exhibits a complex Mo $3d_{5/2}$ peak shape characterized by two components: a sharper, slightly asymmetric main peak at 229.3 eV and a broader, higher-binding-energy feature at 231.0 eV, ascribed to screened and unscreened final states, respectively.[3,6] This characteristic structure tends to vanish in mixed oxide systems, where electronic disorder and reduced conductivity suppress the screened contribution. In such cases, typical of the mixed molybdate samples studied here, the spectra usually display a simplified Mo 3d envelope dominated by unscreened-like peaks.

Deconvolution of the Mo $3d_{5/2}$ region in our samples revealed components at 233.6, 232.4, 230.7, and 229.7 eV. The feature at 233.6 eV is assigned to polymeric Mo–O species ("polymolybdate", PM), while 232.4 eV corresponds to $Mo^{6+}$. Peaks at 230.7 and 229.7 eV fall within the $Mo^{4+}$ binding-energy range. Although the lower-energy feature at ~229.7 eV is slightly higher than the screened $MoO_2$ $3d_{5/2}$ peak typically reported near 229.3 eV, literature variations of ± 0.5-1.0 eV and the frequent absence of distinct screened/unscreened pairs in mixed or disordered oxides support its assignment to $Mo^{4+}$.[3,6] Both species are therefore attributed to $Mo^{4+}$, in agreement with iterative fitting and corroborated by post-reaction XRD results. The contributions likely arise from screened MoC (229.7 eV) and $MoO_2$ (230.7 eV) components.

**$N_2$-Physisorption.** BET surface areas were determined by $N_2$ physisorption at -196 °C using a Quantachrome Quadrasorb Evo instrument. Samples (~0.5 g) were pretreated by removing physisorbed water under vacuum at 120 °C for 2 h. Then the samples were cooled down to -196 °C for equilibrium measurement. The surface area analysis was performed at five different pressures along the isotherm and the results were expressed in $m^2\ g^{-1}$.

**Temperature-Programmed Reduction.** Temperature-programmed reduction (TPR) was carried out using a Quantachrome ChemBET apparatus (Quantachrome, Hook, UK). Samples were pretreated under He at 120 °C for 1 h before recording the reduction profile. The analysis was performed from room temperature to 800 °C under a 10 % $H_2$/Ar flow (50 mL $min^{-1}$) with a heating rate of 10 °C $min^{-1}$.

**Scanning and Transmission Electron Microscopy.** Scanning electron microscopy (SEM) was performed using a Quanta 250 emission field scanning electron microscope, providing information on particle size and morphology. The measurements were operated at an acceleration voltage of 10 kV. Before the analysis, the samples were deposited on carbon tape over a brass support.

High-angle annular dark field (HAADF) images were collected in the scanning transmission electron microscopy (STEM) mode coupled with energy dispersive X-ray spectroscopy (EDS), providing additional insights into particle size and morphology, besides dispersion and spatial composition. The measurements were conducted using a FEI Titan Cubed Themis (Thermo Fischer, 300 kV, point resolution of 0.6 Å) microscope. Samples in powder form were dispersed in isopropyl alcohol by sonication for 1 h, and a single drop of sample was deposited over an ultrathin amorphous carbon-coated gold grid.

**X-ray Total Scattering.** X-ray Total Scattering (TS) measurements were performed at the P02.1 PETRA III beamline at DESY (Hamburg, Germany), using a wavelength of $\lambda = 0.20734$ Å. The powder was packed in 1 mm diameter Kapton capillaries for data collection, and the Rapid Acquisition Pair Distribution Function (RA-PDF) setup was employed.[7] The 2D data were integrated using PyFAI, and the TS data were Fourier transformed to obtain PDFs using PDFgetX3. The raw total scattering data were corrected for background, multiple scattering, container scattering, and Compton scattering using xPDFsuite over the range $0.5 < Q < 17.5$ $Å^{-1}$ using a rpoly value of 1.2 and Qmax,inst of 23.5 $Å^{-1}$.[8] The PDFs were analyzed with real-space Rietveld refinements using PDFgui.[9] The refined parameters included the scale factor, lattice parameters, spherical particle diameter, correlated atomic motion, and isotropic atomic displacement parameters (ADPs). Qdamp and Qbroad values were obtained by refining LaB6 NIST standard. The refinements were carried out by employing single or multiple-phase models with $Cu_3Mo_2O_9$ (ICSD CollCode 59289), MoC (ICSD CollCode 43523), $Cu_2O$ (ICSD CollCode 172174), and Cu (ICSD CollCode 136042).

***Operando* Diffuse Reflectance Infrared Fourier Transform Spectroscopy.** *Operando* diffuse reflectance infrared Fourier transform spectroscopy (DRIFTS) measurements were conducted using a Bruker Vertex 80 spectrometer equipped with a low-volume Harrick reaction cell. Background spectra were first collected using a mirror placed in the sample holder. All spectra were acquired at a resolution of 4 $cm^{-1}$, averaging 64 scans per spectrum unless otherwise specified. Approximately 25 mg of the catalyst was loaded into the DRIFTS cell. A desorption pretreatment was performed by heating the sample from room temperature to 150 °C at a ramp rate of 10 °C $min^{-1}$ under a He flow of 30 mL $min^{-1}$. The sample was held at 150 °C for 30 min to remove weakly adsorbed surface species. After cooling to room temperature, a gas mixture consisting of 44.2 mL $min^{-1}$ of $H_2$ and 5.8 mL $min^{-1}$ of He was passed through a bubbler containing acetone at 22 °C, closely matching the catalytic reaction environment. The sample was then heated to 175 °C at a rate of 10 °C $min^{-1}$ and maintained at this temperature for 1 h. During this period, DRIFT spectra were continuously recorded with a resolution of 4 $cm^{-1}$, averaging 32 scans per spectrum. The gas stream was followed by mass spectrometry using a Pfeiffer ThermoStar GSD 350 T mass spectrometer, following the m/z ratios of 43 for acetone, 29 for propane, 41 for propene, 45 for isopropyl alcohol, and 55 for hexanone.

## Supplementary Figures and Tables

**Table S1.** Specific surface areas (SSA) determined by $N_2$ physisorption experiments of the first-row transition metal molybdate catalysts (MMo).

| Sample | SSA ($m^2$ $g^{-1}$) |
|---|---|
| MnMo | 3.6 |
| FeMo | 9.6 |
| CoMo | 21.6 |
| CuMo | 14.6 |
| ZnMo | 6.4 |

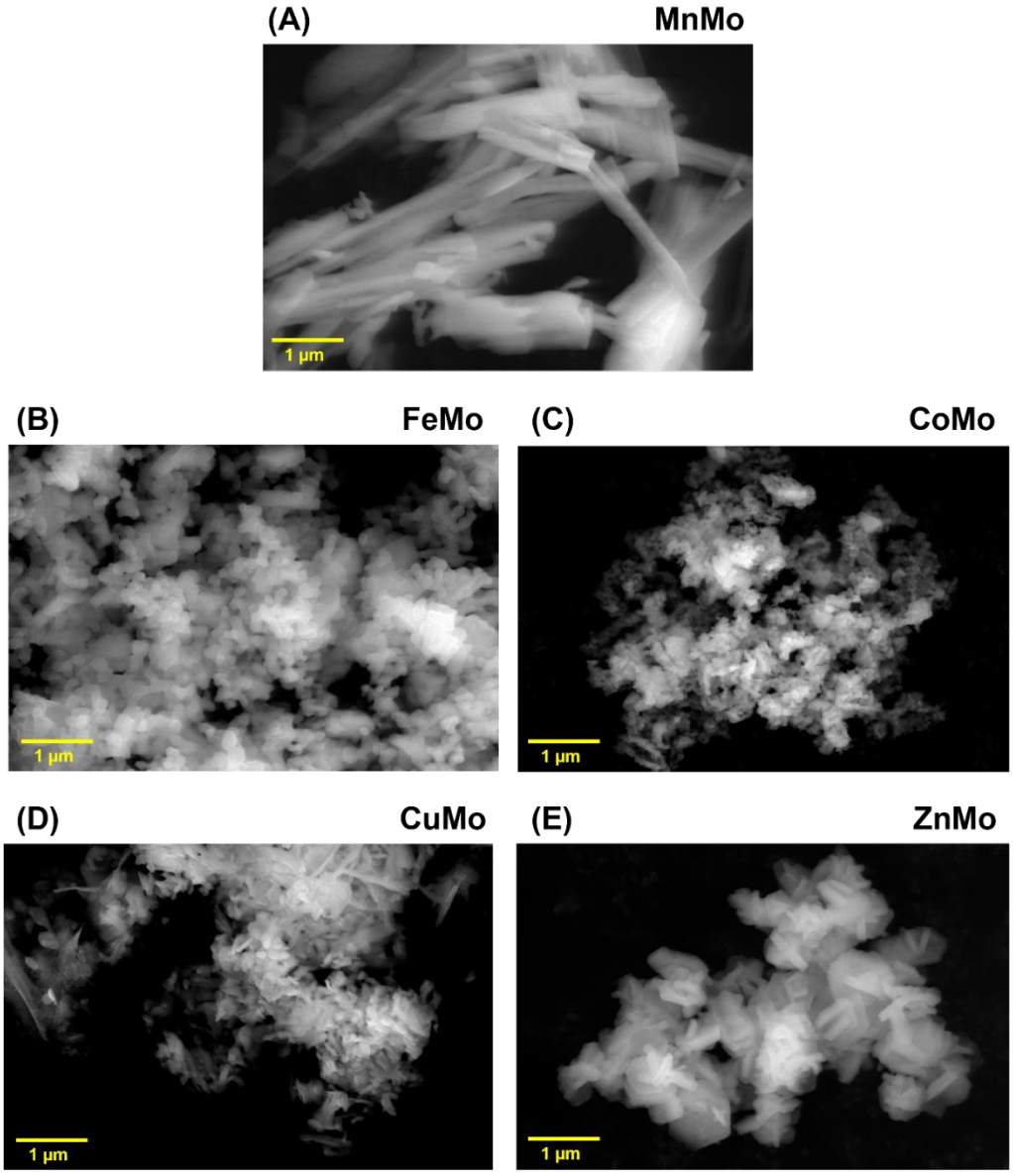


**Figure S1.** SEM images of the first-row transition metal molybdate catalysts: (A) MnMo, (B) FeMo, (C) CoMo, (D) CuMo, and (E) ZnMo.

**Table S2.** Detailed catalytic data obtained under acetone HDO isothermal conditions at 400 °C for the $MoO_3$ nanopowder.

| TOS (min) | Acetone conversion (%) | Products' distribution (%) | | | | | | | |
|---|---|---|---|---|---|---|---|---|---|
| | | $C_1$ | $C_2$ | $C_3E$ | $C_3A$ | $C_4$ | $C_6$ | IPA | $C_6O$ |
| 0 | 27.4 | 0.7 | 1.6 | 72.9 | 8.7 | 8.0 | 2.2 | 0.7 | 5.1 |
| 20 | 48.1 | 0.8 | 0.8 | 68.9 | 12.5 | 3.8 | 7.6 | 0.7 | 5.0 |
| 40 | 43.1 | 0.9 | 0.8 | 67.2 | 13.0 | 3.6 | 6.9 | 0.7 | 6.8 |
| 60 | 38.9 | 1.0 | 1.0 | 65.7 | 13.7 | 3.4 | 6.3 | 0.8 | 8.2 |
| 80 | 35.2 | 0.9 | 1.0 | 64.3 | 14.3 | 3.1 | 6.2 | 0.8 | 9.4 |
| 100 | 33.5 | 1.0 | 1.1 | 63.3 | 14.9 | 2.9 | 5.6 | 0.8 | 10.4 |
| 120 | 31.4 | 1.0 | 1.3 | 62.5 | 14.7 | 2.7 | 4.9 | 0.8 | 12.1 |
| 140 | 29.7 | 1.1 | 1.3 | 61.7 | 14.9 | 2.6 | 3.9 | 0.8 | 13.7 |
| 160 | 28.5 | 1.0 | 1.2 | 60.5 | 15.4 | 2.5 | 3.9 | 0.8 | 14.8 |
| 180 | 27.0 | 1.1 | 1.4 | 59.5 | 15.4 | 2.3 | 3.3 | 0.8 | 16.2 |
| 200 | 25.8 | 1.1 | 1.4 | 58.1 | 16.0 | 2.2 | 3.2 | 0.9 | 17.2 |
| 220 | 25.1 | 1.1 | 1.5 | 57.0 | 16.0 | 2.1 | 3.2 | 0.9 | 18.3 |
| 240 | 24.1 | 1.1 | 1.5 | 56.0 | 16.3 | 2.0 | 2.9 | 1.0 | 19.2 |
| 260 | 23.6 | 1.1 | 1.5 | 55.2 | 16.6 | 1.9 | 2.4 | 1.2 | 20.1 |
| 280 | 23.0 | 1.1 | 1.5 | 54.7 | 16.9 | 1.9 | 1.7 | 1.0 | 21.2 |
| 300 | 22.8 | 1.1 | 1.4 | 53.3 | 18.6 | 1.7 | 1.4 | 1.1 | 21.4 |
| 320 | 21.1 | 1.1 | 1.6 | 54.0 | 16.4 | 1.7 | 1.4 | 1.1 | 22.6 |
| 340 | 21.0 | 1.1 | 1.5 | 52.8 | 17.4 | 1.7 | 1.3 | 1.0 | 23.4 |
| 360 | 21.9 | 1.1 | 1.5 | 51.5 | 17.3 | 1.6 | 1.3 | 1.1 | 24.5 |

**Table S3.** Detailed catalytic data obtained under acetone HDO isothermal conditions at 400 °C for the MnMo catalyst.

| TOS (min) | Acetone conversion (%) | Products' distribution (%) | | | | | |
|---|---|---|---|---|---|---|---|
| | | $C_3E$ | $C_3A$ | IPA | $C_9O$ | $C_6O$ | $CO_2$ |
| 0 | 4.4 | 15.6 | 1.5 | 0.0 | 0.0 | 83.0 | 0.0 |
| 20 | 5.2 | 9.8 | 0.7 | 0.0 | 0.9 | 88.7 | 0.0 |
| 40 | 5.4 | 7.1 | 0.3 | 1.6 | 0.5 | 90.4 | 0.0 |
| 60 | 6.7 | 6.2 | 0.5 | 1.8 | 0.6 | 90.9 | 0.0 |
| 80 | 6.7 | 5.4 | 0.4 | 1.6 | 0.8 | 91.8 | 0.0 |
| 100 | 6.5 | 5.2 | 0.6 | 1.6 | 0.7 | 91.9 | 0.1 |
| 120 | 6.8 | 4.5 | 0.7 | 1.9 | 0.6 | 92.3 | 0.1 |
| 140 | 6.9 | 4.3 | 0.6 | 1.7 | 0.7 | 92.5 | 0.1 |
| 160 | 6.7 | 3.8 | 0.7 | 1.5 | 0.6 | 93.3 | 0.1 |
| 180 | 7.5 | 3.3 | 0.6 | 2.0 | 0.7 | 93.2 | 0.1 |
| 200 | 7.5 | 3.3 | 0.6 | 2.0 | 0.7 | 93.2 | 0.1 |
| 220 | 7.7 | 3.0 | 0.7 | 2.0 | 0.8 | 93.3 | 0.1 |
| 240 | 7.7 | 3.0 | 0.7 | 2.0 | 0.8 | 93.3 | 0.1 |
| 260 | 8.0 | 2.7 | 0.9 | 2.2 | 0.8 | 93.4 | 0.1 |
| 280 | 8.0 | 2.7 | 0.9 | 2.2 | 0.8 | 93.4 | 0.1 |
| 300 | 7.6 | 2.5 | 0.8 | 2.1 | 0.9 | 93.6 | 0.1 |
| 320 | 7.6 | 2.5 | 0.8 | 2.1 | 0.9 | 93.6 | 0.1 |
| 340 | 8.2 | 2.4 | 0.8 | 2.1 | 0.9 | 93.6 | 0.1 |
| 360 | 8.2 | 2.4 | 0.8 | 2.1 | 0.9 | 93.6 | 0.1 |

**Table S4.** Detailed catalytic data obtained under acetone HDO isothermal conditions at 400 °C for the FeMo catalyst.

| TOS (min) | Acetone conversion (%) | Products' distribution (%) | | | | | | | | | | | |
|---|---|---|---|---|---|---|---|---|---|---|---|---|---|
| | | $C_1$ | $C_2$ | $C_3E$ | $C_3A$ | $C_4$ | $C_6$ | $C_9$ | $C_2HO$ | IPA | $C_9O$ | $C_6O$ | $CO_2$ |
| 0 | 38.0 | 0.5 | 0.3 | 39.0 | 3.2 | 8.9 | 21.1 | 6.5 | 0.2 | 0.3 | 4.4 | 15.3 | 0.4 |
| 20 | 45.6 | 0.5 | 0.3 | 39.0 | 3.2 | 8.9 | 21.1 | 6.5 | 0.2 | 0.3 | 4.4 | 15.3 | 0.5 |
| 40 | 52.7 | 0.5 | 0.2 | 35.4 | 3.2 | 9.9 | 20.4 | 7.7 | 0.1 | 0.3 | 9.9 | 11.8 | 0.5 |
| 60 | 55.8 | 0.5 | 0.2 | 34.0 | 3.3 | 9.9 | 21.2 | 7.7 | 0.1 | 0.4 | 10.2 | 12.1 | 0.5 |
| 80 | 56.7 | 0.5 | 0.3 | 32.0 | 3.3 | 9.8 | 21.0 | 8.6 | 0.1 | 0.4 | 10.5 | 13.0 | 0.5 |
| 100 | 55.2 | 0.4 | 0.2 | 29.9 | 4.6 | 9.6 | 20.8 | 8.1 | 0.1 | 0.4 | 10.4 | 15.0 | 0.5 |
| 120 | 55.2 | 0.4 | 0.2 | 29.3 | 4.8 | 10.0 | 21.6 | 8.9 | 0.1 | 0.4 | 11.3 | 12.3 | 0.5 |
| 140 | 53.7 | 0.4 | 0.2 | 28.9 | 4.8 | 9.8 | 21.8 | 8.3 | 0.1 | 0.4 | 11.1 | 13.7 | 0.5 |
| 160 | 52.8 | 0.4 | 0.2 | 28.2 | 5.0 | 9.8 | 21.3 | 8.3 | 0.1 | 0.4 | 11.5 | 14.3 | 0.5 |
| 180 | 52.4 | 0.5 | 0.3 | 28.7 | 4.7 | 10.0 | 21.3 | 8.7 | 0.1 | 0.4 | 11.0 | 14.1 | 0.5 |
| 200 | 52.3 | 0.4 | 0.3 | 28.7 | 4.6 | 9.9 | 21.1 | 7.9 | 0.1 | 0.4 | 11.0 | 15.1 | 0.5 |
| 220 | 51.9 | 0.4 | 0.2 | 27.7 | 5.0 | 9.7 | 20.9 | 8.5 | 0.1 | 0.4 | 10.5 | 16.1 | 0.5 |
| 240 | 51.8 | 0.4 | 0.2 | 28.1 | 5.0 | 9.8 | 21.3 | 7.8 | 0.1 | 0.4 | 10.6 | 15.8 | 0.5 |
| 260 | 52.1 | 0.4 | 0.2 | 27.6 | 5.0 | 9.8 | 21.8 | 7.6 | 0.1 | 0.4 | 10.7 | 15.9 | 0.5 |
| 280 | 51.3 | 0.4 | 0.2 | 27.0 | 5.2 | 9.6 | 21.4 | 7.8 | 0.1 | 0.4 | 10.8 | 16.6 | 0.5 |
| 300 | 50.1 | 0.4 | 0.2 | 27.0 | 5.0 | 9.7 | 21.1 | 7.7 | 0.1 | 0.5 | 10.6 | 17.1 | 0.5 |
| 320 | 50.1 | 0.4 | 0.2 | 26.6 | 5.1 | 9.5 | 21.0 | 7.6 | 0.1 | 0.5 | 10.5 | 18.0 | 0.5 |
| 340 | 48.8 | 0.4 | 0.3 | 26.5 | 5.3 | 9.5 | 21.1 | 7.7 | 0.1 | 0.4 | 10.8 | 17.5 | 0.5 |
| 360 | 49.2 | 0.4 | 0.3 | 26.0 | 5.3 | 9.4 | 20.8 | 7.7 | 0.1 | 0.4 | 11.1 | 18.0 | 0.5 |

**Table S5.** Detailed catalytic data obtained under acetone HDO isothermal conditions at 400 °C for the CoMo catalyst.

| TOS (min) | Acetone conversion (%) | Products' distribution (%) | | | | | | | | | | | |
|---|---|---|---|---|---|---|---|---|---|---|---|---|---|
| | | $C_1$ | $C_2$ | $C_3E$ | $C_3A$ | $C_4$ | $C_6$ | $C_9$ | $C_2HO$ | IPA | $C_9O$ | $C_6O$ | $CO_2$ |
| 0 | 15.8 | 0.3 | 0.1 | 17.4 | 0.9 | 3.9 | 2.1 | 2.0 | 0.1 | 0.0 | 2.5 | 70.6 | 0.2 |
| 20 | 26.6 | 0.5 | 0.1 | 28.0 | 1.7 | 9.7 | 4.5 | 4.5 | 0.2 | 0.3 | 7.5 | 42.4 | 0.5 |
| 40 | 48.2 | 0.7 | 0.3 | 40.0 | 2.9 | 14.6 | 14.8 | 4.7 | 0.2 | 0.5 | 9.0 | 11.6 | 0.7 |
| 60 | 63.4 | 0.7 | 0.3 | 39.5 | 3.4 | 13.2 | 22.0 | 7.6 | 0.1 | 0.6 | 7.2 | 4.7 | 0.6 |
| 80 | 63.6 | 0.8 | 0.4 | 38.1 | 4.2 | 12.7 | 22.3 | 8.0 | 0.1 | 0.6 | 7.2 | 5.0 | 0.6 |
| 100 | 63.9 | 0.8 | 0.4 | 37.7 | 3.8 | 13.0 | 22.6 | 8.0 | 0.1 | 0.6 | 7.5 | 4.9 | 0.6 |
| 120 | 62.2 | 0.9 | 0.4 | 38.6 | 3.4 | 12.3 | 22.2 | 8.2 | 0.1 | 0.6 | 7.7 | 4.9 | 0.6 |
| 140 | 62.1 | 0.9 | 0.4 | 39.0 | 3.4 | 12.4 | 22.6 | 7.6 | 0.1 | 0.6 | 7.8 | 4.6 | 0.6 |
| 160 | 62.8 | 1.0 | 0.4 | 39.0 | 3.7 | 11.9 | 22.3 | 7.5 | 0.1 | 0.6 | 7.7 | 5.2 | 0.5 |
| 180 | 62.3 | 1.1 | 0.4 | 39.5 | 3.8 | 11.3 | 21.7 | 7.8 | 0.1 | 0.6 | 7.5 | 5.6 | 0.5 |
| 200 | 61.8 | 1.1 | 0.4 | 40.0 | 3.6 | 11.3 | 21.8 | 7.5 | 0.1 | 0.6 | 7.5 | 5.7 | 0.5 |
| 220 | 62.0 | 1.2 | 0.4 | 39.9 | 3.6 | 11.1 | 22.2 | 7.6 | 0.1 | 0.6 | 7.8 | 5.1 | 0.5 |
| 240 | 62.5 | 1.2 | 0.4 | 41.9 | 3.3 | 11.3 | 21.0 | 7.0 | 0.1 | 0.5 | 7.9 | 4.8 | 0.5 |
| 260 | 62.2 | 1.3 | 0.5 | 41.0 | 3.8 | 10.6 | 21.6 | 7.4 | 0.1 | 0.5 | 7.5 | 5.3 | 0.4 |
| 280 | 62.9 | 1.3 | 0.4 | 41.1 | 3.7 | 10.8 | 21.9 | 7.1 | 0.2 | 0.5 | 7.6 | 4.9 | 0.4 |
| 300 | 62.0 | 1.3 | 0.4 | 42.2 | 2.9 | 10.6 | 21.5 | 7.4 | 0.1 | 0.5 | 7.5 | 5.1 | 0.4 |
| 320 | 61.7 | 1.3 | 0.4 | 41.7 | 3.5 | 10.5 | 21.5 | 6.9 | 0.1 | 0.5 | 8.0 | 4.9 | 0.4 |
| 340 | 60.0 | 1.4 | 0.4 | 42.9 | 3.3 | 10.2 | 21.2 | 6.9 | 0.1 | 0.5 | 7.9 | 4.8 | 0.4 |
| 360 | 60.1 | 1.4 | 0.4 | 43.0 | 3.3 | 10.5 | 21.6 | 6.9 | 0.1 | 0.6 | 7.6 | 4.2 | 0.4 |

**Table S6.** Detailed catalytic data obtained under acetone HDO isothermal conditions at 400 °C for the CuMo catalyst.

| TOS (min) | Acetone conversion (%) | Products' distribution (%) | | | | | | | | | | | |
|---|---|---|---|---|---|---|---|---|---|---|---|---|---|
| | | $C_1$ | $C_2$ | $C_3E$ | $C_3A$ | $C_4$ | $C_6$ | $C_9$ | $C_2HO$ | IPA | $C_9O$ | $C_6O$ | $CO_2$ |
| 0 | 64.8 | 0.5 | 2.7 | 65.1 | 5.6 | 15.3 | 6.5 | 1.1 | 0.9 | 0.2 | 1.6 | 0.1 | 0.3 |
| 20 | 63.5 | 0.6 | 2.7 | 64.1 | 3.1 | 16.9 | 7.4 | 1.3 | 0.6 | 0.2 | 1.0 | 1.8 | 0.3 |
| 40 | 63.5 | 0.8 | 2.6 | 59.4 | 2.7 | 19.8 | 8.4 | 2.1 | 0.4 | 0.3 | 1.4 | 1.8 | 0.4 |
| 60 | 57.8 | 0.8 | 2.5 | 60.0 | 1.5 | 19.4 | 9.4 | 2.5 | 0.5 | 0.3 | 1.9 | 2.1 | 0.4 |
| 80 | 54.2 | 0.8 | 2.4 | 60.5 | 1.1 | 19.6 | 8.4 | 2.0 | 0.5 | 0.4 | 2.1 | 2.1 | 0.4 |
| 100 | 50.2 | 0.8 | 2.4 | 60.2 | 1.3 | 19.3 | 8.8 | 1.8 | 0.5 | 0.4 | 2.2 | 2.1 | 0.4 |
| 120 | 50.7 | 0.8 | 2.3 | 59.9 | 1.0 | 19.6 | 8.7 | 2.0 | 0.5 | 0.3 | 2.5 | 2.1 | 0.4 |
| 140 | 48.8 | 0.8 | 2.3 | 60.6 | 0.7 | 19.3 | 8.7 | 1.9 | 0.5 | 0.3 | 2.6 | 2.3 | 0.0 |
| 160 | 46.6 | 0.8 | 2.3 | 59.9 | 1.3 | 19.5 | 8.7 | 2.0 | 0.5 | 0.3 | 2.5 | 2.2 | 0.0 |
| 180 | 45.5 | 0.8 | 2.2 | 59.2 | 1.3 | 19.5 | 8.9 | 1.9 | 0.5 | 0.3 | 2.9 | 2.1 | 0.3 |
| 200 | 44.2 | 0.8 | 2.2 | 59.1 | 1.0 | 19.7 | 8.8 | 1.9 | 0.5 | 0.3 | 3.0 | 2.4 | 0.4 |
| 220 | 43.6 | 0.8 | 2.2 | 58.7 | 0.9 | 20.1 | 8.7 | 2.0 | 0.5 | 0.3 | 3.2 | 2.3 | 0.4 |
| 240 | 41.7 | 0.8 | 2.2 | 58.3 | 1.0 | 19.5 | 9.0 | 2.3 | 0.5 | 0.3 | 3.0 | 2.7 | 0.4 |
| 260 | 40.8 | 0.8 | 2.1 | 58.4 | 0.7 | 20.0 | 8.9 | 2.3 | 0.5 | 0.3 | 3.3 | 2.3 | 0.4 |
| 280 | 39.1 | 0.8 | 2.2 | 58.8 | 1.1 | 19.7 | 8.8 | 1.7 | 0.5 | 0.3 | 3.2 | 2.6 | 0.4 |
| 300 | 40.2 | 0.9 | 2.1 | 58.1 | 1.1 | 20.2 | 8.7 | 1.7 | 0.5 | 0.3 | 3.6 | 2.5 | 0.4 |
| 320 | 37.6 | 0.8 | 2.1 | 57.7 | 1.4 | 20.2 | 8.9 | 1.8 | 0.5 | 0.3 | 3.6 | 2.4 | 0.4 |
| 340 | 38.5 | 0.9 | 2.1 | 57.1 | 1.7 | 20.3 | 8.9 | 1.9 | 0.5 | 0.2 | 4.0 | 2.1 | 0.4 |
| 360 | 37.7 | 0.9 | 2.1 | 58.2 | 1.4 | 16.9 | 9.6 | 2.1 | 0.6 | 0.3 | 4.4 | 3.2 | 0.4 |

**Table S7.** Detailed catalytic data obtained under acetone HDO isothermal conditions at 400 °C for the ZnMo catalyst.

| TOS (min) | Acetone conversion (%) | Products' distribution (%) | | | | | | | | | | | |
|---|---|---|---|---|---|---|---|---|---|---|---|---|---|
| | | $C_1$ | $C_2$ | $C_3E$ | $C_3A$ | $C_4$ | $C_6$ | $C_9$ | $C_2HO$ | IPA | $C_9O$ | $C_6O$ | $CO_2$ |
| 0 | 11.9 | 0.0 | 0.0 | 53.7 | 1.2 | 2.3 | 4.9 | 0.0 | 0.4 | 1.1 | 5.3 | 30.9 | 0.2 |
| 20 | 9.6 | 0.2 | 0.3 | 40.6 | 1.0 | 3.8 | 7.1 | 2.6 | 0.4 | 0.9 | 3.6 | 39.2 | 0.2 |
| 40 | 17.8 | 0.2 | 0.2 | 52.2 | 1.5 | 7.6 | 9.0 | 1.5 | 0.4 | 0.5 | 4.4 | 22.3 | 0.3 |
| 60 | 41.6 | 0.2 | 0.3 | 58.8 | 2.7 | 10.1 | 15.2 | 2.1 | 0.2 | 0.7 | 3.2 | 6.2 | 0.3 |
| 80 | 55.2 | 0.3 | 0.6 | 50.4 | 6.1 | 11.7 | 19.6 | 2.5 | 0.2 | 0.9 | 3.7 | 3.6 | 0.4 |
| 100 | 56.2 | 0.3 | 0.6 | 44.9 | 8.0 | 12.0 | 20.6 | 2.9 | 0.2 | 1.0 | 4.0 | 5.1 | 0.4 |
| 120 | 55.5 | 0.3 | 0.6 | 41.2 | 10.0 | 11.6 | 19.8 | 2.7 | 0.2 | 1.1 | 3.9 | 8.3 | 0.4 |
| 140 | 54.7 | 0.3 | 0.7 | 40.2 | 8.4 | 12.4 | 19.8 | 3.0 | 0.2 | 1.1 | 4.2 | 8.4 | 0.5 |
| 160 | 50.1 | 0.3 | 0.6 | 39.9 | 7.8 | 12.8 | 19.8 | 3.0 | 0.2 | 1.0 | 4.5 | 8.7 | 0.5 |
| 180 | 51.1 | 0.3 | 0.7 | 38.3 | 7.8 | 12.6 | 21.8 | 3.1 | 0.2 | 1.1 | 4.4 | 9.4 | 0.4 |
| 200 | 51.4 | 0.3 | 0.7 | 37.1 | 7.9 | 12.9 | 21.6 | 3.9 | 0.2 | 1.0 | 4.7 | 9.2 | 0.5 |
| 220 | 45.2 | 0.3 | 0.7 | 36.1 | 8.3 | 13.0 | 21.7 | 3.5 | 0.2 | 1.1 | 4.8 | 9.9 | 0.5 |
| 240 | 42.4 | 0.3 | 0.7 | 35.9 | 8.2 | 12.7 | 20.8 | 3.4 | 0.2 | 1.1 | 4.4 | 11.7 | 0.5 |
| 260 | 43.2 | 0.3 | 0.7 | 35.2 | 8.0 | 12.8 | 20.8 | 4.0 | 0.2 | 1.1 | 4.5 | 12.0 | 0.5 |
| 280 | 44.5 | 0.3 | 0.6 | 34.4 | 8.5 | 13.3 | 21.5 | 4.2 | 0.2 | 1.0 | 4.8 | 10.4 | 0.5 |
| 300 | 45.5 | 0.3 | 0.6 | 33.9 | 8.4 | 13.3 | 20.9 | 5.0 | 0.2 | 1.1 | 5.0 | 10.8 | 0.5 |
| 320 | 44.2 | 0.3 | 0.7 | 34.6 | 7.7 | 13.3 | 21.4 | 3.6 | 0.3 | 1.1 | 4.9 | 11.6 | 0.5 |
| 340 | 44.4 | 0.3 | 0.6 | 33.6 | 8.2 | 13.1 | 21.1 | 3.2 | 0.2 | 1.2 | 4.9 | 13.2 | 0.5 |
| 360 | 48.4 | 0.3 | 0.7 | 34.8 | 8.4 | 13.8 | 22.1 | 3.4 | 0.2 | 1.1 | 5.3 | 9.4 | 0.5 |

**Table S8.** Detailed catalytic data obtained for acetone HDO reaction as a function of temperature (300 to 400 °C) for the $MoO_3$ nanopowder.

| Temperature (°C) | Acetone conversion (%) | Products' distribution (%) | | | | | | | | | |
|---|---|---|---|---|---|---|---|---|---|---|---|
| | | $C_1$ | $C_2$ | $C_3E$ | $C_3A$ | $C_4$ | $C_6$ | $C_9$ | IPA | $C_9O$ | $C_6O$ |
| 300 | 3.9 | 0.0 | 0.0 | 49.0 | 2.8 | 0.0 | 0.0 | 0.0 | 0.0 | 0.0 | 45.6 |
| 320 | 6.0 | 0.0 | 0.0 | 41.9 | 2.3 | 0.0 | 0.0 | 0.0 | 0.0 | 5.7 | 48.9 |
| 340 | 7.4 | 0.0 | 0.0 | 42.5 | 3.0 | 0.0 | 0.0 | 0.0 | 0.0 | 6.4 | 45.2 |
| 360 | 8.2 | 0.0 | 0.0 | 38.7 | 4.1 | 1.9 | 0.0 | 0.0 | 0.0 | 5.5 | 47.2 |
| 380 | 18.7 | 0.8 | 1.3 | 42.9 | 31.3 | 6.1 | 1.6 | 0.5 | 0.0 | 1.6 | 13.7 |
| 400 | 25.9 | 0.8 | 1.8 | 52.3 | 23.1 | 6.6 | 2.8 | 0.8 | 0.0 | 2.4 | 9.3 |

**Table S9.** Detailed catalytic data obtained for acetone HDO reaction as a function of temperature (300 to 400 °C) for the MnMo catalyst.

| Temperature (°C) | Acetone conversion (%) | Products' distribution (%) | | | | | | | | |
|---|---|---|---|---|---|---|---|---|---|---|
| | | $C_3E$ | $C_3A$ | $C_4$ | $C_6$ | $C_9$ | IPA | $C_9O$ | $C_6O$ | $CO_2$ |
| 300 | 3.3 | 57.0 | 0.0 | 0.0 | 0.0 | 0.0 | 0.0 | 0.0 | 35.7 | 7.3 |
| 320 | 4.5 | 58.1 | 0.0 | 0.0 | 0.0 | 0.0 | 0.0 | 0.0 | 33.4 | 8.5 |
| 340 | 5.2 | 49.4 | 0.0 | 3.5 | 0.0 | 0.0 | 0.0 | 0.0 | 40.2 | 7.0 |
| 360 | 11.3 | 35.2 | 3.4 | 7.6 | 1.6 | 0.0 | 0.0 | 0.0 | 50.0 | 2.1 |
| 380 | 39.5 | 33.2 | 3.3 | 9.7 | 5.4 | 6.1 | 0.0 | 9.4 | 32.3 | 0.6 |
| 400 | 66.3 | 42.5 | 3.8 | 12.4 | 11.9 | 7.4 | 0.9 | 9.1 | 11.2 | 0.8 |

**Table S10.** Detailed catalytic data obtained for acetone HDO reaction as a function of temperature (300 to 400 °C) for the FeMo catalyst.

| Temperature (°C) | Acetone conversion (%) | Products' distribution (%) | | | | | | | |
|---|---|---|---|---|---|---|---|---|---|
| | | $C_1$ | $C_3E$ | $C_3A$ | $C_4$ | IPA | $C_9O$ | $C_6O$ | $CO_2$ |
| 300 | 3.8 | 0.0 | 54.4 | 0.0 | 0.0 | 5.5 | 3.5 | 35.7 | 0.8 |
| 320 | 5.0 | 0.0 | 43.7 | 0.0 | 0.0 | 6.6 | 2.9 | 46.2 | 0.5 |
| 340 | 5.2 | 0.0 | 40.3 | 0.0 | 0.0 | 9.5 | 2.8 | 46.9 | 0.4 |
| 360 | 4.6 | 0.0 | 32.1 | 0.0 | 0.0 | 6.5 | 7.4 | 53.7 | 0.2 |
| 380 | 7.2 | 0.0 | 11.5 | 0.9 | 1.2 | 2.2 | 3.9 | 80.1 | 0.1 |
| 400 | 8.9 | 0.3 | 7.6 | 1.7 | 2.9 | 1.6 | 4.4 | 81.3 | 0.2 |

**Table S11.** Detailed catalytic data obtained for acetone HDO reaction as a function of temperature (300 to 400 °C) for the CoMo catalyst.

| Temperature (°C) | Acetone conversion (%) | Products' distribution (%) | | | | | | | | | | |
|---|---|---|---|---|---|---|---|---|---|---|---|---|
| | | $C_1$ | $C_2$ | $C_3E$ | $C_3A$ | $C_4$ | $C_6$ | $C_9$ | $C_2HO$ | $C_9O$ | $C_6O$ | $CO_2$ |
| 300 | 4.0 | 3.4 | 3.7 | 9.0 | 0.4 | 0.4 | 1.3 | 9.5 | 0.9 | 1.3 | 67.8 | 2.2 |
| 320 | 5.1 | 2.9 | 3.1 | 9.6 | 0.5 | 0.7 | 1.9 | 8.8 | 0.7 | 0.8 | 69.2 | 1.9 |
| 340 | 6.4 | 1.8 | 2.0 | 8.4 | 0.5 | 1.2 | 2.0 | 7.7 | 0.6 | 0.7 | 73.9 | 1.2 |
| 360 | 7.3 | 1.3 | 1.6 | 9.3 | 0.5 | 1.0 | 1.7 | 6.6 | 0.4 | 1.3 | 75.4 | 1.0 |
| 380 | 9.2 | 0.5 | 0.6 | 10.7 | 0.4 | 1.9 | 0.8 | 3.8 | 0.1 | 9.7 | 72.4 | 0.3 |
| 400 | 18.6 | 0.5 | 0.3 | 18.7 | 0.8 | 5.1 | 1.6 | 3.4 | 0.1 | 4.0 | 65.1 | 0.3 |

**Table S12.** Detailed catalytic data obtained for acetone HDO reaction as a function of temperature (300 to 400 °C) for the CuMo catalyst.

| Temperature (°C) | Acetone conversion (%) | Products' distribution (%) | | | | | | | | | | |
|---|---|---|---|---|---|---|---|---|---|---|---|---|
| | | $C_1$ | $C_2$ | $C_3E$ | $C_3A$ | $C_4$ | $C_6$ | $C_9$ | IPA | $C_9O$ | $C_6O$ | $CO_2$ |
| 300 | 93.8 | 0.0 | 0.0 | 86.8 | 6.2 | 1.5 | 5.3 | 0.0 | 0.1 | 0.0 | 0.0 | 0.0 |
| 320 | 64.7 | 0.0 | 0.5 | 84.4 | 4.1 | 2.7 | 7.1 | 0.0 | 0.1 | 0.7 | 0.3 | 0.0 |
| 340 | 57.4 | 0.0 | 1.0 | 75.3 | 3.1 | 7.2 | 9.2 | 0.3 | 0.2 | 2.8 | 0.8 | 0.1 |
| 360 | 46.3 | 0.2 | 2.7 | 61.1 | 2.8 | 16.1 | 9.3 | 0.8 | 0.3 | 4.7 | 1.9 | 0.2 |
| 380 | 48.9 | 0.3 | 3.1 | 59.2 | 2.8 | 18.6 | 8.8 | 1.0 | 0.3 | 3.3 | 2.3 | 0.2 |
| 400 | 61.4 | 0.5 | 3.0 | 61.3 | 1.9 | 18.9 | 9.7 | 1.2 | 0.3 | 2.1 | 1.7 | 0.3 |

**Table S13.** Detailed catalytic data obtained for acetone HDO reaction as a function of temperature (300 to 400 °C) for the ZnMo catalyst.

| Temperature (°C) | Acetone conversion (%) | Products' distribution (%) | | | | | | | | | |
|---|---|---|---|---|---|---|---|---|---|---|---|
| | | $C_1$ | $C_2$ | $C_3E$ | $C_3A$ | $C_4$ | $C_6$ | IPA | $C_9O$ | $C_6O$ | $CO_2$ |
| 300 | 6.5 | 0.0 | 0.0 | 14.5 | 0.0 | 0.6 | 0.0 | 6.8 | 9.0 | 69.2 | 0.0 |
| 320 | 4.4 | 0.0 | 0.0 | 30.6 | 0.0 | 1.0 | 0.0 | 5.6 | 5.4 | 57.4 | 0.0 |
| 340 | 4.6 | 0.0 | 0.0 | 36.8 | 0.0 | 1.1 | 0.0 | 4.3 | 5.9 | 51.8 | 0.0 |
| 360 | 4.1 | 0.0 | 0.0 | 37.4 | 0.0 | 1.7 | 0.0 | 3.2 | 5.2 | 52.5 | 0.0 |
| 380 | 8.1 | 0.3 | 0.0 | 41.6 | 0.0 | 5.0 | 1.4 | 1.3 | 4.1 | 45.9 | 0.2 |
| 400 | 42.3 | 0.3 | 0.4 | 69.1 | 4.7 | 9.0 | 7.9 | 0.4 | 2.0 | 5.3 | 0.3 |

**Table S14.** Surface elemental composition and oxidation states of Mo and M species in fresh and post-reaction MMo catalysts obtained from XPS analysis. Quantification is expressed in atomic percent. The Mo oxidation states were deconvoluted into Mo(6+) and Mo(4+). The oxidation states of the transition metal cations refer to M(2+), M(3+) for Fe*, and M(0).

| Sample | | Quantification (at.%) | | | | | | | | Atomic ratios | | | |
|---|---|---|---|---|---|---|---|---|---|---|---|---|---|
| | | C | O | PM | Mo(6+) | Mo(4+) $MoO_2$ | Mo(4+) MoC | M(2+)* | M(0) | Nominal Mo/M | Experimental Mo/M | Nominal (Mo+M)/O | Experimental (Mo+M)/O |
| MnMo | Fresh | 23.04 | 49.03 | 1.30 | 17.51 | - | - | 9.12 | - | 1.0 | 2.1 | 0.5 | 0.6 |
| | Post-reaction | 24.29 | 66.88 | 0.87 | 3.70 | 0.15 | - | 4.11 | - | 1.0 | 1.1 | 0.5 | 0.1 |
| FeMo | Fresh | 19.72 | 53.43 | 0.24 | 20.08 | - | - | 6.53 | - | 1.5 | 3.1 | 0.4 | 0.5 |
| | Post-reaction | 29.17 | 59.94 | 0.35 | 5.45 | 0.83 | 0.43 | 3.82 | | 1.5 | 1.8 | 0.4 | 0.2 |
| CoMo | Fresh | 30.01 | 46.44 | 0.74 | 14.17 | - | - | 8.63 | - | 1.0 | 1.7 | 0.5 | 0.5 |
| | Post-reaction | 35.08 | 54.52 | 0.63 | 3.00 | 1.48 | - | 5.28 | - | 1.0 | 0.9 | 0.5 | 0.2 |
| CuMo | Fresh | 26.37 | 46.53 | 0.52 | 13.80 | - | - | 12.78 | - | 0.7 | 1.1 | 0.6 | 0.6 |
| | Post-reaction | 25.9 | 62.62 | 0.62 | 3.18 | 0.72 | - | 6.16 | 0.80 | 0.7 | 0.6 | 0.6 | 0.2 |
| ZnMo | Fresh | 20.59 | 50.40 | 0.07 | 17.19 | - | - | 11.75 | - | 1.0 | 1.5 | 0.5 | 0.6 |
| | Post-reaction | 34.52 | 53.93 | - | 3.18 | 2.70 | 0.13 | 5.54 | - | 1.0 | 1.1 | 0.5 | 0.2 |

**Table S15.** Surface atomic fractions of Mo and M species in post-reaction MMo catalysts derived from XPS analysis. The Mo oxidation states were deconvoluted into Mo(6+) and Mo(4+). The oxidation states of the transition metal cations refer to M(2+), M(3+) for Fe*, and M(0).

| Post-reaction sample | Atomic Fraction | | | | |
|---|---|---|---|---|---|
| | Mo | | | M | |
| | PM | Mo(6+) | Mo(4+) | M(2+)* | M(0) |
| MnMo | 0.18 | 0.78 | 0.03 | 1.00 | 0.00 |
| FeMo | 0.05 | 0.77 | 0.18 | 1.00 | 0.00 |
| CoMo | 0.12 | 0.59 | 0.29 | 1.00 | 0.00 |
| CuMo | 0.14 | 0.70 | 0.16 | 0.88 | 0.12 |
| ZnMo | 0.12 | 0.59 | 0.29 | 1.00 | 0.00 |

**Table S16.** Detailed catalytic data obtained for acetone HDO reaction as a function of temperature (100 to 300 °C) for the CuMo catalyst.

| Temperature (°C) | Acetone conversion (%) | Products' distribution (%) | | | | | | | | | |
|---|---|---|---|---|---|---|---|---|---|---|---|
| | | $C_3E$ | $C_3A$ | $C_4$ | $C_6$ | $C_9$ | $C_2HO$ | IPA | $C_9O$ | $C_6O$ | $CO_2$ |
| 100 | 6.0 | 0.0 | 0.0 | 0.0 | 0.0 | 0.0 | 7.7 | 28.5 | 0.0 | 62.9 | 0.9 |
| 150 | 6.9 | 0.0 | 0.0 | 0.0 | 0.0 | 0.0 | 8.6 | 67.3 | 0.0 | 22.6 | 1.4 |
| 200 | 6.8 | 35.1 | 0.0 | 0.0 | 0.0 | 0.0 | 1.6 | 24.3 | 2.2 | 35.1 | 1.7 |
| 250 | 81.2 | 84.4 | 4.1 | 0.2 | 9.0 | 0.5 | 0.0 | 1.6 | 0.2 | 0.1 | 0.0 |
| 300 | 80.4 | 84.2 | 3.4 | 1.5 | 9.9 | 0.6 | 0.0 | 0.2 | 0.3 | 0.0 | 0.0 |

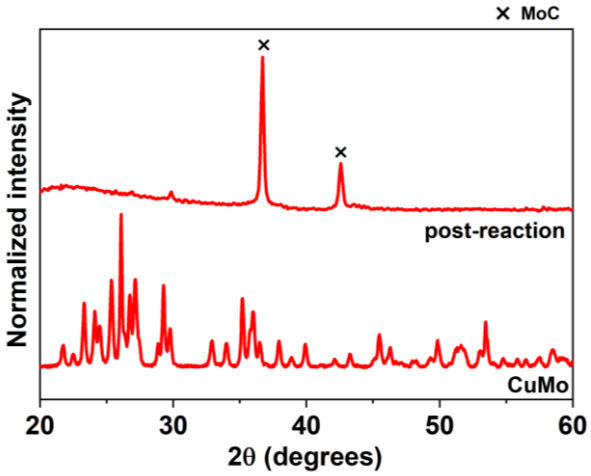


**Figure S2.** Powder XRD patterns of the fresh and post-reaction CuMo catalyst (100 to 300 °C).

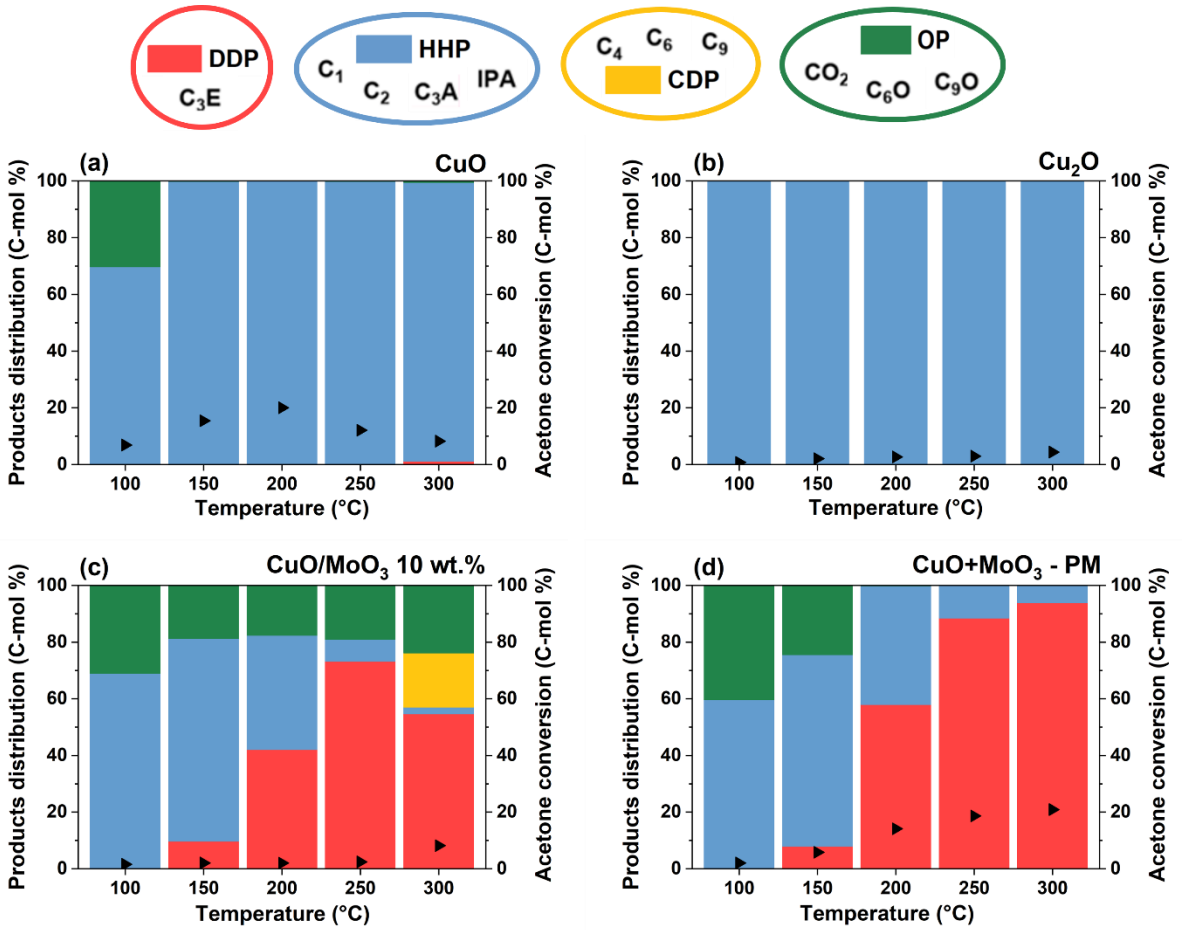


**Figure S3.** Products' distribution (colored) and conversion (black triangles) for acetone HDO reaction over Cu-based catalysts: (a) CuO, (b) $Cu_2O$, (c) $CuO/MoO_3$ 10 wt.%, and (d) $CuO+MoO_3$ - PM. The temperature-dependent tests were carried out from 100 to 300 °C, isothermal every 50 °C, total TOS: ~3 h. WHSV = 7.32 $g_{acetone}\ g_{catalyst}^{-1}\ h^{-1}$. Feed: 2.4 mL $min^{-1}$ acetone, 51 mL $min^{-1}$ $H_2$, balance He. Total flow: 100 mL $min^{-1}$.

**Table S17.** Summary of the catalytic data obtained for acetone HDO reaction at 300 °C for the Cu-based catalysts: CuO, $Cu_2O$, $CuO/MoO_3$ 10 wt.%, and $CuO+MoO_3$ – physical mixture.

| Sample | Acetone conversion (%) | Acetone consumption rates ($mmol_{acetone}\ g_{cat}^{-1}\ h^{-1}$) | Products' distribution (%) | | | |
|---|---|---|---|---|---|---|
| | | | HHP* | DDP* | CDP* | OP* |
| CuO | 8.2 | 10 | 98.2 | 1.2 | 0.0 | 0.6 |
| $Cu_2O$ | 4.4 | 6 | 100.0 | 0.0 | 0.0 | 0.0 |
| $CuO/MoO_3$ 10 wt.% | 8.2 | 10 | 7.0 | 38.6 | 15.3 | 39.1 |
| $CuO+MoO_3$ | 20.9 | 26 | 6.1 | 93.8 | 0.0 | 0.1 |

* HHP: hydrogenation/hydrogenolysis products, DDP: direct deoxygenation products, CDP: coupling deoxygenation products, OP: oxygenation products.

**Table S18.** Detailed catalytic data obtained for acetone HDO reaction as a function of temperature (100 to 300 °C) for the CuO catalyst.

| Temperature (°C) | Acetone conversion (%) | Products' distribution (%) | | | |
|---|---|---|---|---|---|
| | | $C_3E$ | $C_2HO$ | IPA | $C_6O$ |
| 100 | 6.9 | 0.0 | 7.6 | 69.7 | 22.7 |
| 150 | 15.4 | 0.0 | 0.2 | 99.8 | 0.0 |
| 200 | 20.0 | 0.0 | 0.1 | 99.9 | 0.0 |
| 250 | 12.1 | 0.0 | 0.2 | 99.8 | 0.0 |
| 300 | 8.2 | 1.2 | 0.6 | 98.2 | 0.0 |

**Table S19.** Detailed catalytic data obtained for acetone HDO reaction as a function of temperature (100 to 300 °C) for the $Cu_2O$ catalyst.

| Temperature (°C) | Acetone conversion (%) | Products' distribution (%) |
|---|---|---|
| | | IPA |
| 100 | 0.7 | 100.0 |
| 150 | 2.1 | 100.0 |
| 200 | 2.7 | 100.0 |
| 250 | 3.0 | 100.0 |
| 300 | 4.4 | 100.0 |

**Table S20.** Detailed catalytic data obtained for acetone HDO reaction as a function of temperature (100 to 300 °C) for the $CuO/MoO_3$ 10 wt.% catalyst.

| Temperature (°C) | Acetone conversion (%) | Products' distribution (%) | | | | | | | | | |
|---|---|---|---|---|---|---|---|---|---|---|---|
| | | $C_3E$ | $C_3A$ | $C_4$ | $C_6$ | $C_9$ | $C_2HO$ | IPA | $C_9O$ | $C_6O$ | $CO_2$ |
| 100 | 1.6 | 0.0 | 0.0 | 0.0 | 0.0 | 0.0 | 6.4 | 76.3 | 0.0 | 16.2 | 1.1 |
| 150 | 2.0 | 14.4 | 0.0 | 0.0 | 0.0 | 0.0 | 2.3 | 54.0 | 9.9 | 18.7 | 0.7 |
| 200 | 2.0 | 45.4 | 0.0 | 0.7 | 5.0 | 0.0 | 0.8 | 23.0 | 20.6 | 4.3 | 0.1 |
| 250 | 2.4 | 45.6 | 0.0 | 0.9 | 12.5 | 1.1 | 0.2 | 5.3 | 21.3 | 13.1 | 0.1 |
| 300 | 8.2 | 38.6 | 6.2 | 3.6 | 11.2 | 0.5 | 0.2 | 0.8 | 10.2 | 28.7 | 0.1 |

**Table S21.** Detailed catalytic data obtained for acetone HDO reaction as a function of temperature (100 to 300 °C) for the $CuO+MoO_3$ – physical mixture catalyst.

| Temperature (°C) | Acetone conversion (%) | Products' distribution (%) | | | | |
|---|---|---|---|---|---|---|
| | | $C_3E$ | $C_2HO$ | IPA | $C_6O$ | $CO_2$ |
| 100 | 2.0 | 0.0 | 5.8 | 59.6 | 32.1 | 2.6 |
| 150 | 5.8 | 7.9 | 2.4 | 67.6 | 21.1 | 1.0 |
| 200 | 14.1 | 57.9 | 0.1 | 42.0 | 0.0 | 0.1 |
| 250 | 18.6 | 88.4 | 0.1 | 11.5 | 0.0 | 0.0 |
| 300 | 20.9 | 93.8 | 0.1 | 6.1 | 0.0 | 0.0 |

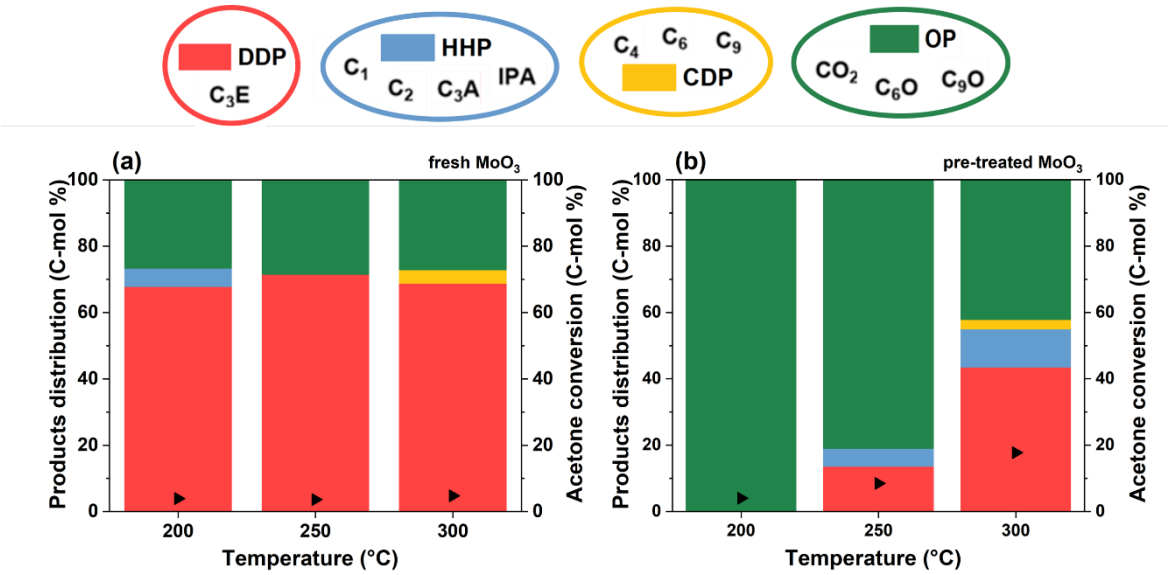


**Figure S4.** Products' distribution (colored) and conversion (black triangles) for acetone HDO reaction over fresh and pre-treated $MoO_3$ catalysts. The later was exposed to acetone HDO reaction conditions at 400 °C for 30 min prior to the catalytic test. The temperature-dependent tests were carried out from 100 to 300 °C, isothermal every 50 °C, total TOS: ~2 h. WHSV = 7.32 $g_{acetone}$ $g_{catalyst}^{-1}$ $h^{-1}$. Feed: 2.4 mL $min^{-1}$ acetone, 51 mL $min^{-1}$ $H_2$, balance He. Total flow: 100 mL $min^{-1}$.

**Table S22.** Summary of the catalytic data obtained for acetone HDO reaction as a function of temperature (100 to 300 °C) for the fresh and pre-treated $MoO_3$ catalysts.

| Sample | Temperature (°C) | Acetone conversion (%) | Acetone consumption rates ($mmol_{acetone}$ $g_{cat}^{-1}$ $h^{-1}$) | Products' distribution (%) | | | |
|---|---|---|---|---|---|---|---|
| | | | | HHP* | DDP* | CDP* | OP* |
| Fresh $MoO_3$ | 200 | 3.9 | 5 | 5.6 | 0 | 67.8 | 26.6 |
| | 250 | 3.6 | 5 | 0 | 0 | 71.5 | 28.5 |
| | 300 | 4.7 | 6 | 0 | 4.1 | 68.8 | 27.1 |
| Pre-treated $MoO_3$ | 200 | 4.0 | 5 | 0 | 0 | 0 | 100.0 |
| | 250 | 8.5 | 11 | 5.4 | 13.6 | 0 | 81.0 |
| | 300 | 17.8 | 22 | 11.5 | 43.5 | 2.8 | 42.2 |

* HHP: hydrogenation/hydrogenolysis products, DDP: direct deoxygenation products, CDP: coupling deoxygenation products, OP: oxygenation product.

**Table S23.** Surface elemental composition in post-reaction CuMo catalysts (without diluent) obtained from XPS analysis. Quantification is expressed in atomic percent. The Mo oxidation states were deconvoluted into Mo(6+) and Mo(4+) species. Cu(2+) and Cu(0) refer to the oxidation states of copper.

| Sample | Quantification (at.%) | | | | | | | | Atomic ratios | | | |
|---|---|---|---|---|---|---|---|---|---|---|---|---|
| | C | O | PM | Mo(6+) | Mo(4+) $MoO_2$ | Mo(4+) MoC | Cu(2+) | Cu(0) | Nominal Mo/Cu | Experimental Mo/Cu | Nominal (Mo+Cu)/O | Experimental (Mo+Cu)/O |
| CuMo – 175 °C | 35.37 | 43.64 | 0.56 | 5.23 | - | - | 13.18 | 2.04 | 0.7 | 0.4 | 0.6 | 0.5 |
| CuMo – 200 °C | 33 | 44.12 | 0.53 | 7.63 | 0.35 | - | 11.66 | 2.72 | 0.7 | 0.6 | 0.6 | 0.5 |
| CuMo – 300 °C | 29.18 | 46.48 | 2.20 | 9.09 | 2.01 | - | 5.09 | 5.95 | 0.7 | 1.2 | 0.6 | 0.5 |

**Table S24.** PDF real space Rietveld refinement parameters of the short- and medium-range order for fresh CuMo and pre-treated samples under acetone HDO reaction conditions at 200 and 300 °C employing $Cu_3Mo_2O_9$, MoC, and Cu phases as model.

| Rw | Phase model | Scale factor | δ2 (Å$^2$) | a lattice parameter (Å) | b lattice parameter (Å) | c lattice parameter (Å) | $ADP_{Cu}$ (Å$^2$) | $ADP_{Mo}$ (Å$^2$) | $ADP_{O/C}$ (Å$^2$) |
|---|---|---|---|---|---|---|---|---|---|
| 0.18 | $Cu_3Mo_2O_9$ | 0.48 | 2.6 | 7.66 | 6.88 | 14.62 | 0.0064 | 0.0052 | 0.0339 |
| 0.38 | $Cu_3Mo_2O_9$ | 0.40 | 3.2 | 8.93 | 6.70 | 13.54 | 0.0144 | 0.0156 | 0.1874 |
| | MoC | 0.08 | 2.1 | 4.30 | 4.30 | 4.30 | - | 0.0141 | 0.0966 |
| 0.20 | Cu | 0.22 | 3.6 | 3.62 | 3.62 | 3.62 | 0.0079 | - | - |
| 0.18 | $Cu_3Mo_2O_9$ | 0.43 | - | 7.68 | 6.87 | 14.62 | 0.0092 | 0.0061 | 0.0322 |
| 0.25 | MoC | 0.12 | - | 4.27 | 4.27 | 4.27 | - | 0.0390 | 0.1761 |
| | Cu | 0.01 | - | 3.62 | 3.62 | 3.62 | 0.0074 | - | - |

* Short- to medium-range order real space Rietveld refinements primarily reflect local structural order rather than the full particle size, thus mean particle size diameter was not included in the refined parameters table.

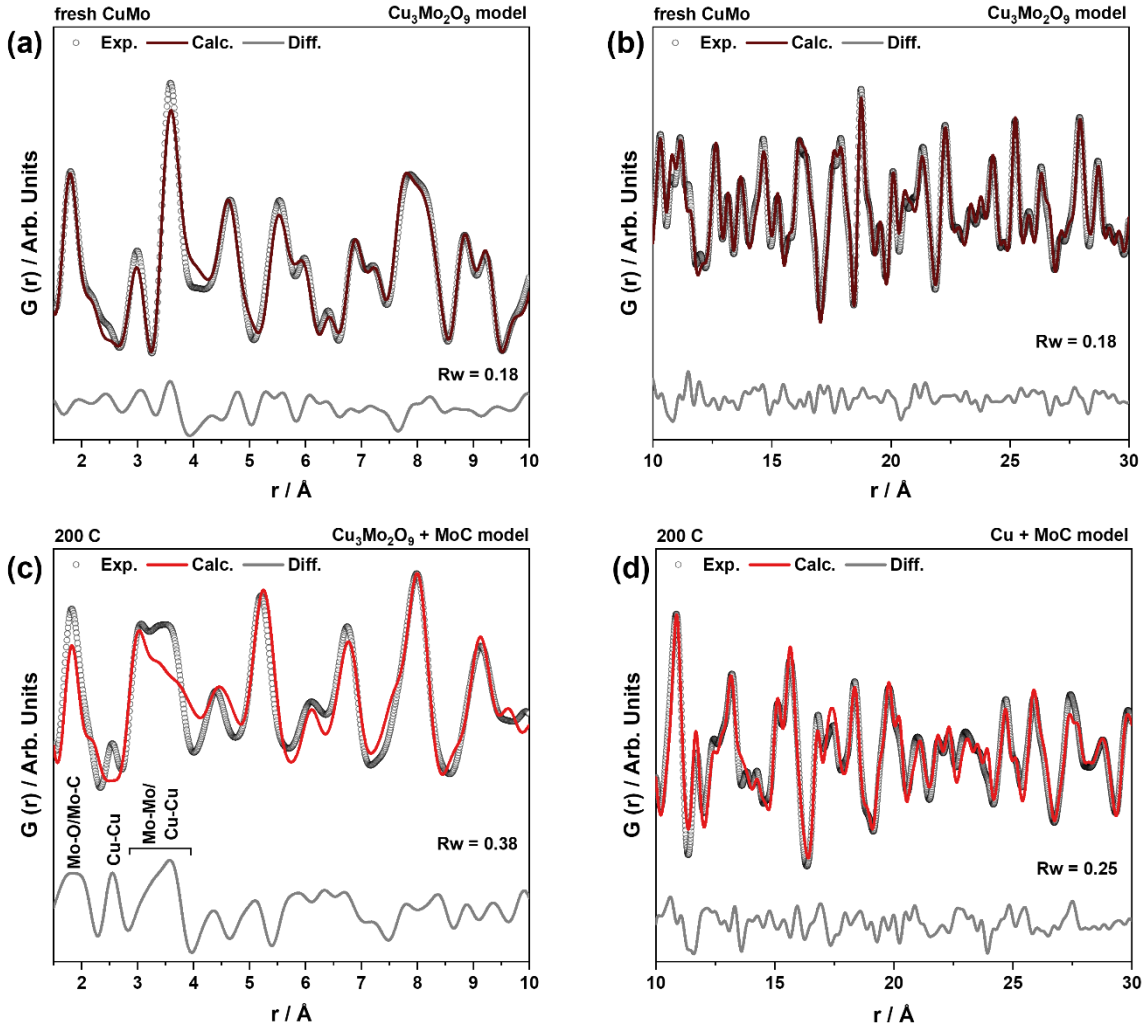


**Figure S5.** Short- and medium- to long-range order PDF refinements of (a,b) fresh CuMo and (c,d) after pre-treatment under acetone HDO reaction conditions at 200 °C. $Cu_3Mo_2O_9$, MoC, and Cu phases were employed as models for the refinements, as indicated at the top right of each graph.

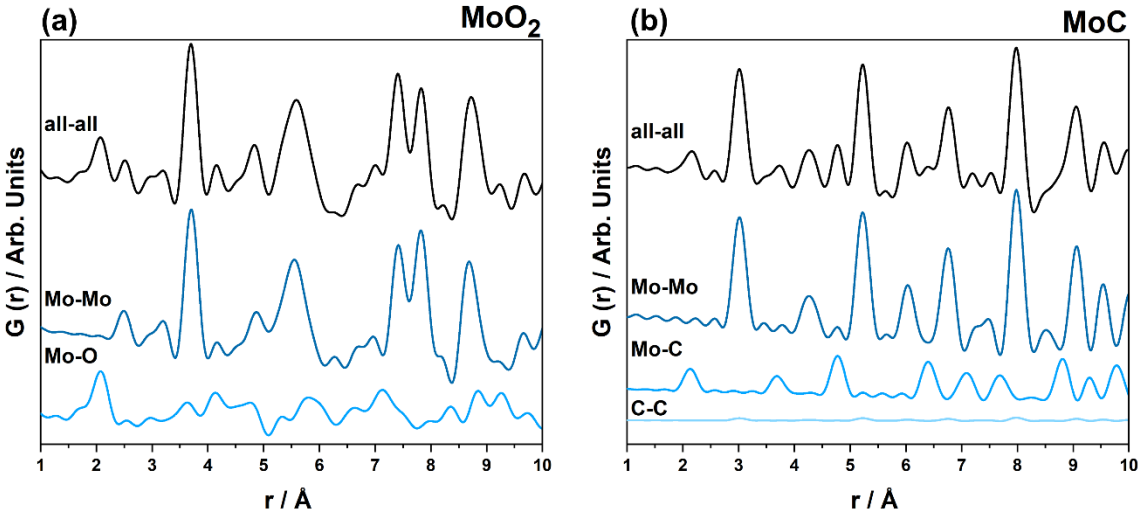


**Figure S6.** Simulated short-range order PDFs of (a) $MoO_2$ (space group $P2_1/c$, ICSD collCode 152316) and (b) MoC (space group *Fm-3m*, ICSD collCode 43523).

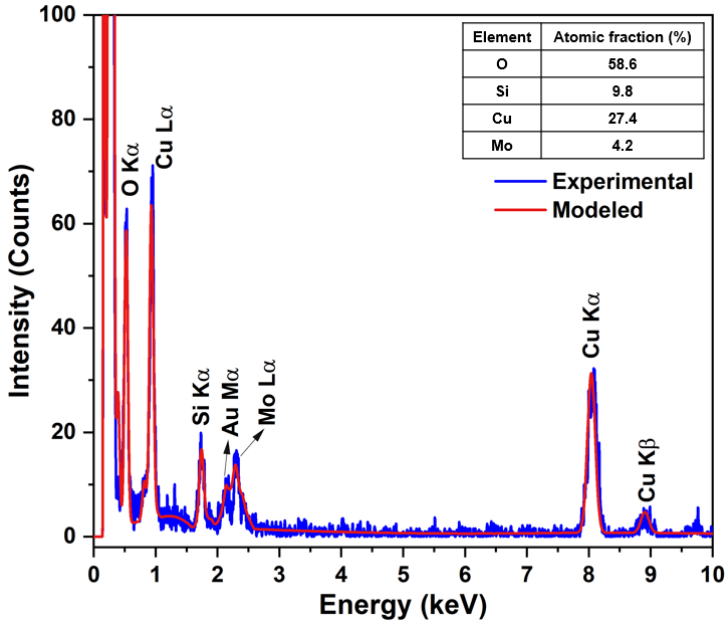


**Figure S7.** EDS spectrum obtained from the TEM analysis and elements atomic fractions related to CuMo catalyst after pre-treatment under acetone HDO reaction conditions at 300 °C.

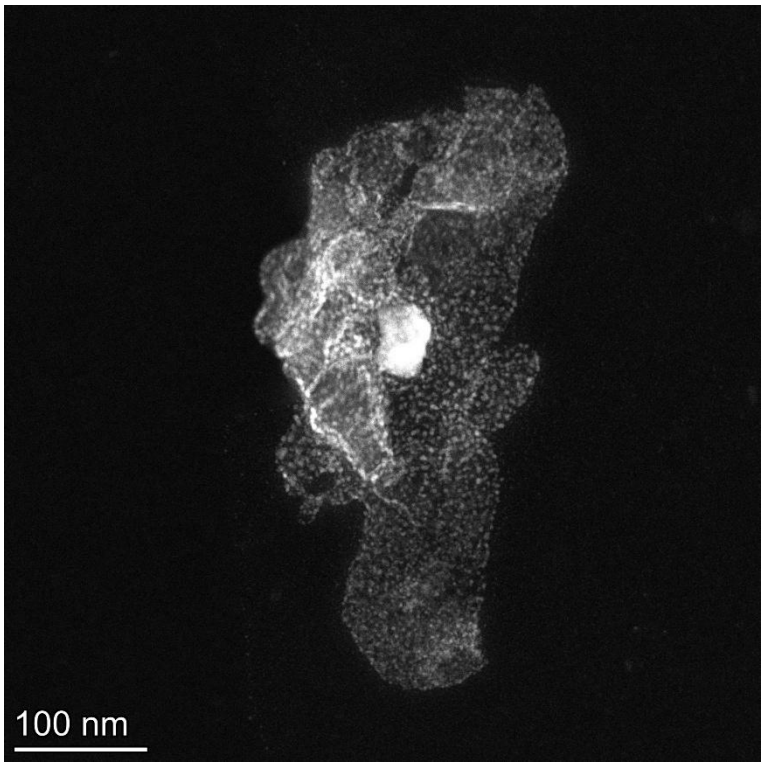


**Figure S8.** TEM image of the CuMo catalyst after pre-treatment under acetone HDO reaction conditions at 300 °C.

## References


1 https://icsd.fiz-karlsruhe.de/index.xhtml.

2 N. Fairley, V. Fernandez, M. Richard-Plouet, C. Guillot-Deudon, J. Walton, E. Smith, D. Flahaut, M. Greiner, M. Biesinger, S. Tougaard, D. Morgan and J. Baltrusaitis, *Applied Surface Science Advances*, 2021, **5**, 100112.

3 J. Baltrusaitis, B. Mendoza-Sanchez, V. Fernandez, R. Veenstra, N. Dukstiene, A. Roberts and N. Fairley, *Appl. Surf. Sci.*, 2015, **326**, 151–161.

4 D. J. Morgan, M. A. Isaacs and A. Graf, *Surface and Interface Analysis*, 2025, **57**, 816–821.

5 https://srdata.nist.gov/.

6 D. O. Scanlon, G. W. Watson, D. J. Payne, G. R. Atkinson, R. G. Egdell and D. S. L. Law, *The Journal of Physical Chemistry C*, 2010, **114**, 4636–4645.

7 G. Ashiotis, A. Deschildre, Z. Nawaz, J. P. Wright, D. Karkoulis, F. E. Picca and J. Kieffer, *J. Appl. Crystallogr.*, 2015, **48**, 510–519.

8 P. Juhás, T. Davis, C. L. Farrow and S. J. L. Billinge, *J. Appl. Crystallogr.*, 2013, **46**, 560–566.

9 C. L. Farrow, P. Juhas, J. W. Liu, D. Bryndin, E. S. Božin, J. Bloch, T. Proffen and S. J. L. Billinge, *Journal of Physics: Condensed Matter*, 2007, **19**, 335219.